JOURNAL OF MATERIALS SCIENCE 31 (1996) 6449–6454

Soft chemical synthesis and characterization of lithium nickel oxide electrode materials

X. XIAO*, Y. XU‡
Department of Materials Science and Engineering, and ‡Department of Chemistry, Tsinghua University, Beijing, 100084, People's Republic of China

Soft chemistry was used to prepare ordered nanophase $Li_{0.6}NiO_2$ electrode materials by completing the oxidation of Ni^{2+} to Ni^{3+} and/or Ni^{4+} species with H_2O_2 oxidant during solution reactions at 50–60 °C and evaporation at 105–150 °C rather than during sintering. Both elemental analysis and electron spectroscopy for chemical analysis (ESCA) results indicate that oxidation was completed. The deconvoluted ESCA spectra of nickel ions exhibited a semi-quantitative ratio of $Ni^{4+}:Ni^{3+}=60:40$ which presented no significant change with increase of sintering time. After sintering for up to 11 h at 700 °C, ordered $Li_{0.61}Ni_{0.96}O_{2.0}$ ceramics were formed (R3*m*, $a_0=0.2837$ nm, $c_0=1.417$ nm). Distribution of the crystallite size was in the range of 80–200 nm. As sintering times were increased, the crystallite shapes exhibited a more distinct morphology, and the ordering degree of the cations was enhanced, while the conductivity was sharply enhanced up to $2.0\times10^{-1}\,\Omega^{-1}\,cm^{-1}$ at 30 °C. Compared to conventional ceramic and solution methods, the ordered nanophase $Li_{0.61}Ni_{0.96}O_{2.0}$ ceramics was obtained at 700 °C with shorter sintering times ($\approx$11 h).

1. Introduction

Layered lithium nickelate compound, as a fast-ion conductor, exhibits a two dimensionality of structural and physical properties. It is one of the best candidates for electrode materials [1, 2], and shows high potential for applications and a commercial tendency for 4 V rechargeable lithium batteries because of the following advantages [3, 4]. (a) Compared to conventional Ni/Cd and PbO_2/Pb rechargeable batteries, lithium nickelate battery has a much higher energy density and longer cycle life with no poison elements such as cadmium and lead; (b) Compared to analogous batteries, such as lithium cobalt oxide battery, it is also cheaper [5–7].

Preparation of lithium nickelate ceramics is by two major routes: (a) ceramic preparation based on solid-state reactions in oxygen is a conventional method both in laboratories and in industry, but this requires high reaction temperatures (usually greater than 700 °C) and long sintering times (usually greater than 30 h) [8]; (b) solution synthesis is homogeneous at the atomic level, but it is difficult to oxidize Ni^{2+} ions to Ni^{3+} and Ni^{4+} ions during sintering [9]. This causes two problems: (a) high energy assumptions, and (b) difficult to prepare nanophase lithium nickelate materials due to high reaction temperatures or long sintering times.

The aim of this study was to synthesize nanophase lithium nickelate electrode materials using reduced sintering times and low reaction temperature [10, 11]. A soft chemical method was proposed to achieve this goal, i.e. the oxidation of Ni^{2+} to Ni^{3+} and Ni^{4+} was completed during solution reaction and evaporation prior to sintering. Lithium nickel oxides ($Li_{0.6}NiO_2$) were chosen in this study because, in the "rocking–chair" type of rechargeable batteries, electrochemical reaction is conducted through intercalation–deintercalation of Li^+ ion between the layered cathode and anode materials. Thus, study on synthesis, structure and conductivity of $Li_{0.6}NiO_2$ ($x \leq 1$) is the key to understanding the mechanism of the electrochemical reactions. The present paper reports the results.

2. Experimental procedure

Preparations of lithium nickelate ($Li_{0.6}NiO_2$) ceramics were based on the following oxidation reactions

$$Ni^{2+}(CH_3COO)^-_{2\,(sol)} + xLi^+(CH_3COO)^-_{(sol)}$$

$$+ \text{excess } H_2O_2 \xrightarrow{50\text{–}60\,^\circ C} \text{dark green solution}$$

$$+ CO_2\uparrow \xrightarrow{105\text{–}150\,^\circ C} \text{dried black ppt}$$

$$(Li^+ + Ni^{3+} + Ni^{4+}) \quad (1)$$

Analytical reagents [$Ni(CH_3COO)_2\cdot4H_2O$], [$Li(CH_3COO)\cdot2H_2O$] and H_2O_2 (30%) were purchased from the Beijing Chemical Factory. Nickel

*Author to whom all correspondence should be addressed.

0022–2461

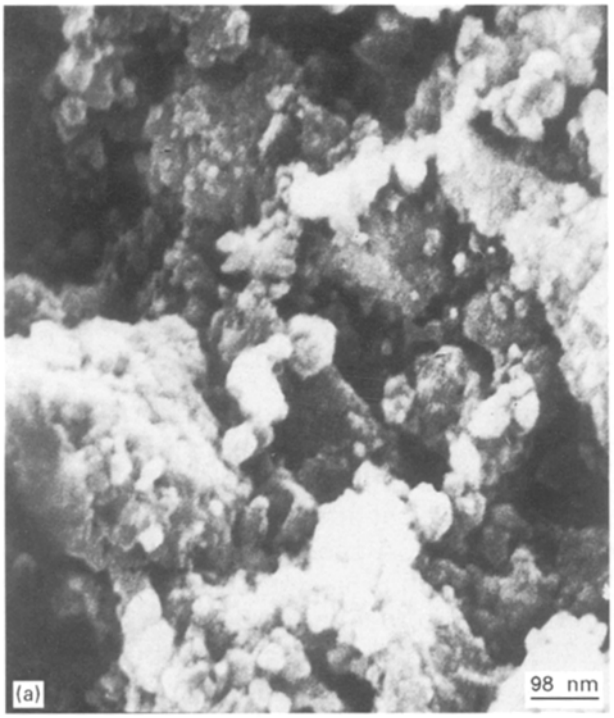

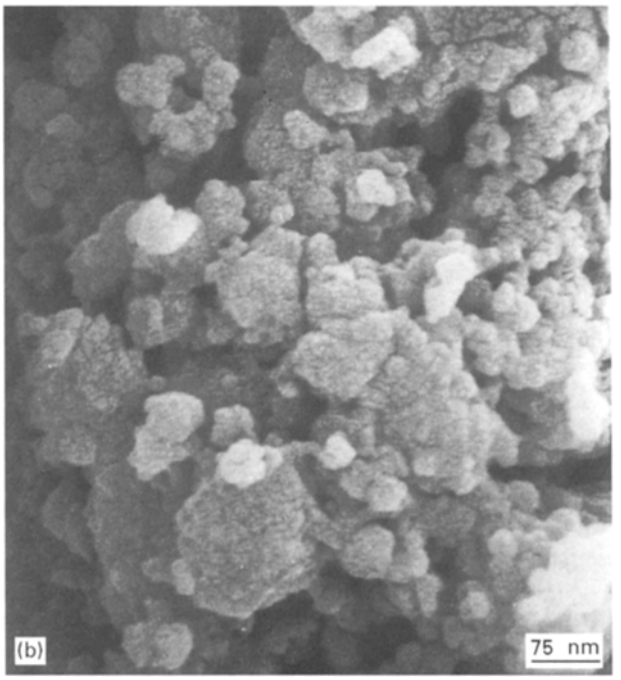

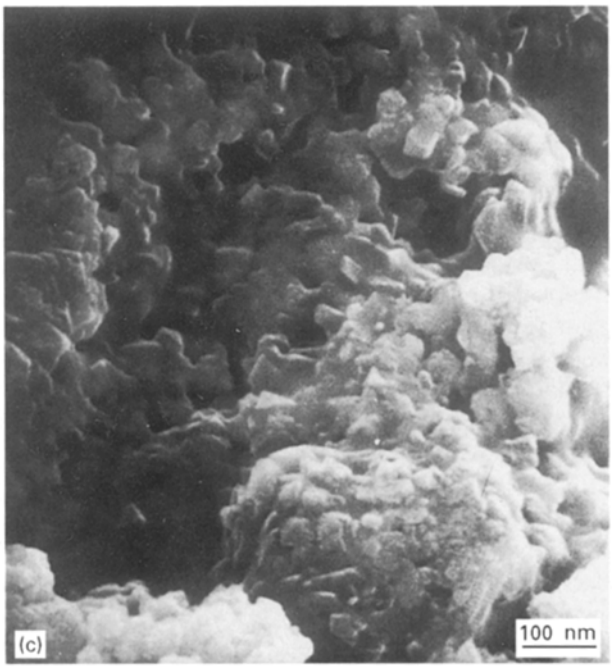

Figure 1 Scanning electron micrographs of the lithium nickel oxides synthesized through the soft chemical routes: (a) the black precipitates before sintering, (b) the lithium nickelate ceramics after 4 h sintering, and (c) after 11 h sintering.

acetate crystallites of about 17.7 g were dissolved in distilled H_2O, and 30 ml H_2O_2 was added. The solution was stirred and heated at 50–60 °C, while much foam was produced. The colour of the solution changed from green to dark green in 20 min. Then about 4.4 g lithium acetate crystallites were dissolved into the solution followed by a further 30 ml H_2O_2. The solution was evaporated to dryness at 105–150 °C, while the oxidation was strongly carried out. An additional 10 ml H_2O_2 was added to obtain black precipitates. The black precipitates were ground and pressed as pellets with dimensions of 10 mm diameter × 1.2 mm. The pellets were sintered in air at 700 °C for 1, 2, 3, 4 and 11 h, respectively.

Surface morphology and particle sizes were observed by using an Hitachi S-450 scanning electron microscope (SEM) with a working voltage of 25 kV. The samples were mounted on a metal holder, and coated with carbon. Elemental analysis on all products were carried out using a WFS-1B atomic absorption spectrometer for lithium and a gravimetric method (dimethyl glyoxime as the chelating agent) for nickel. Structure analysis was performed with a Rigaku D/max-IIIB X-ray diffractometer (XRD). The accelerating voltage and current were 30 kV and 20 mA, respectively, with a scan speed of $4° \text{ min}^{-1}$. Order–disorder states were further studied with the aid of a Perkin–Elmer Fourier transform–infrared (FT–IR) 1650 infrared spectrometer with a resolution at 4 cm^{-1} and a scan speed of 16 min^{-1}. Mixed nickel valences were determined by Perkin-Elmer PHI 5100 electron spectroscopy for chemical analysis (ESCA). The MgK_α (1253.6 eV) anode was used as the X-ray source. The operation voltage and power were 15 kV and 400 W, respectively. The tilt angle was chosen as 45°, and the resolution was 0.4 eV. Deconvolution of the composite spectra was carried out by means of a least-square curve-fitting program. A d.c. resistivity–temperature measurement unit was employed to measure conductivities in the range of $30 \leq T \leq 300$ °C.

3. Results and discussion

3.1. Morphology

Scanning electron micrographs indicate that the unsintered black precipitates were agglomerates of ultrafine particles ranging from 80–140 nm (Fig. 1a). However, rhombohedral crystallites began to show up after sintering, and their morphologies became more distinct as the sintering times were increased at 700 °C

TABLE I Elemental analysis of the lithium nickel oxides sintered at 700 °C

Elements	Sintering time		
	0 (h)	4 h	11 h
Li (wt %)[a]	4.46 ± 0.30	4.56 ± 0.30	4.54 ± 0.24
Ni (wt %)[b]	60.98 ± 0.87	60.81 ± 0.83	60.92 ± 0.85
Experimental formula	$Li_{0.60}Ni_{0.96}O_{2.0}$[c]	$Li_{0.61}Ni_{0.96}O_{2.0}$	$Li_{0.61}Ni_{0.96}O_{2.0}$

[a] Analysed by WFS-1B atomic absorption spectrometer (mean ± 2σ).
[b] Analysed by gravimetric method with dimethyl glyoxime as the chelating agent (mean ± 2σ).
[c] Hypothetical formula for the multiple-phase precipitates.

TABLE II X-ray diffraction data of the lithium nickel oxides sintered at 700 °C

Sample						Reference [13]		
0 (h)		4 h		11 h				
2θ (deg)	I/I_0	2θ (deg)	I/I_0	2θ (deg)	I/I_0	2θ (deg)	I/I_0	hkl
				18.8	17	18.6	16	003
31.6	8	31.6	8					002[a]
				36.6	12	36.4	6	101
37.1	58	37.6	45	38.8	58	37.9	20	102 or 006
43.1	95	43.6	100	44.9	100	44.0	100	104
44.3	100							200[a]
51.7	36							100[a]
62.7	40	63.9	50	64.9	75	64.0	35	018
75.2	20							?[b]
75.5	19							?[b]
76.1	20	76.3	18	77.9	20	76.9	10	116
79.2	18	80.2	16	81.9	20	84.1	10	0012

[a] XRD data of Ni_2O_3 from *The X-ray powder Diffraction File*, **14-483**.
[b] Assigned for Li_xNiO_2?

(Fig. 1b and c). The product sintered for 11 h had the most distinct rhombohedral crystallites. The crystallite sizes tended to increase as the sintering time increased, and ranged in size from 80–200 nm, suggesting the formation of nanophase materials [12].

3.2. Elemental analysis

Elemental analysis data are listed in Table I. Each sample was analysed three times to obtain a mean value and standard deviation. The results clearly indicate that the oxidations of Ni^{2+} to Ni^{3+} and/or Ni^{4+} ions were completed during the solution reactions at 50–60 °C and evaporation at 105–150 °C, rather than during sintering (Table I). Even though it was difficult to oxidize Ni^{2+} to Ni^{3+} and/or Ni^{4+} ions, the reaction temperatures at 50–60 °C and the evaporation at 105–150 °C (strong oxidation) played very important roles in the oxidation. The elemental analysis uniformly provided an experimental chemical formula as $Li_{0.61}Ni_{0.96}O_{2.0}$ for all products under different sintering durations. This further confirmed the achievement of the oxidation reactions in solution. It should be noticed that this formula may only be assigned for those sintered samples (Table I), and not for the unsintered black precipitates which might be a mixture of oxides.

3.3. Crystallographic structure

Multiple phases were determined in the XRD patterns of the unsintered precipitates (Table II). Evidence for rhombohedral lithium nickelate (Li_xNiO_2) and hexagonal Ni_2O_3 was seen, as well as several peaks which could not be assigned. For the pellets with 11 h sintering, rhombohedral $Li_{0.61}Ni_{0.96}O_{2.0}$ crystallites were formed ($R3m$, $a_0 = 0.2837$ nm and $c_0 = 1.417$ nm). The unit-cell parameters are smaller than those ($a_0 = 0.2946$ nm and $c_0 = 1.429$ nm) of the sample sintered for 4 h (Fig. 2). This implies a higher ordering of the cations in the former than that in the latter [13]. The increased ratios of intensities of $I_{(003)}/I_{(104)}$ and/or $I_{(101)}/I_{(102,006)}$ are also considered to be indicators of cation ordering [14]. In Fig. 2, the cation ordering peaks at (003) and (101) could not be observed for the samples sintered for less than 11 h, implying that the cation ordering was enhanced as the sintering times increased.

Apparently, after only 1 h sintering, changes in the XRD patterns were seen, indicating the beginning of the transformation to layered $Li_{0.61}Ni_{0.96}O_{2.0}$ (Table II). On the other hand, the ordering peaks at (003) and (101) could not be observed for the products sintered up to 4 h, they could only be identified for the products sintered for 11 h (Fig. 2). This indicates that the reaction appeared to be completed

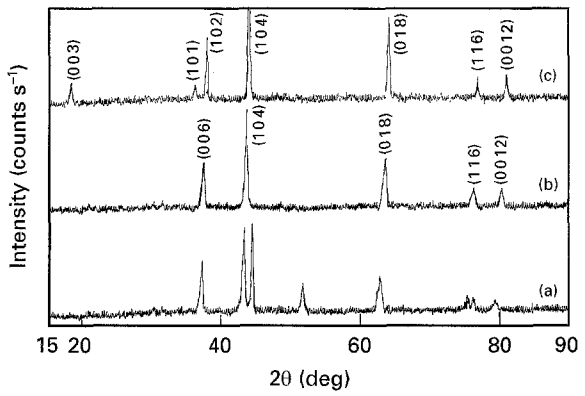

Figure 2 Changes of XRD diffraction patterns of the lithium nickel oxides as sintering times were increased: (a) the precipitates before sintering; (b) after 4 h sintering; and (c) after 11 h sintering, where the ordering peaks (003) and (101) can be observed.

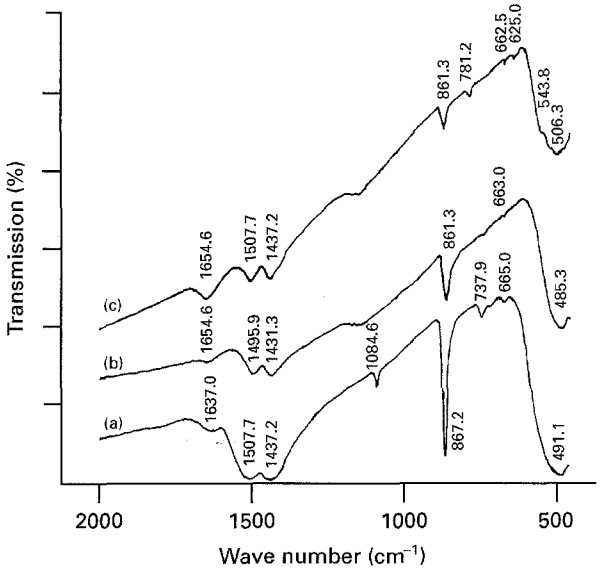

Figure 3 FT–IR spectra of the lithium nickel oxides: (a) the sample before sintering: (b) after 4 h sintering; and (c) after 11 h sintering, where all the four vibration bands show up.

for obtaining the ordered $Li_{0.61}Ni_{0.96}O_{2.0}$ after 11 h sintering [8, 9, 14].

3.4. FT–IR spectra

The cation ordering as a function of sintering times was further studied by an infrared spectrometer. Based on analysis of group theory, there are four infrared active vibrations for the D_{3d} group [14]. Since the LiO_2^- and NiO_2^- structure layers are separated in the lithium nickelate compound, four vibration bands can be identified in the range of 400–700 cm^{-1} for the NiO_2-layer and four in the range of 200–400 cm^{-1} for the LiO_2-layer, respectively. For the pellets sintered for 4 h, there were only two bands at 485.3 and 663.0 cm^{-1}, reflecting the formation of disordered lithium nickel oxides. For the pellets sintered for 11 h, there were four bands attributed to NiO_2^- structure at 502.9, 543.8, 625.0 and 662.5 cm^{-1}. Obviously, such infrared characteristics reveal that the degree of ordering of cations in the latter was higher than that in the former, confirming that the cation ordering was enhanced with increasing sintering time (Fig. 3). The

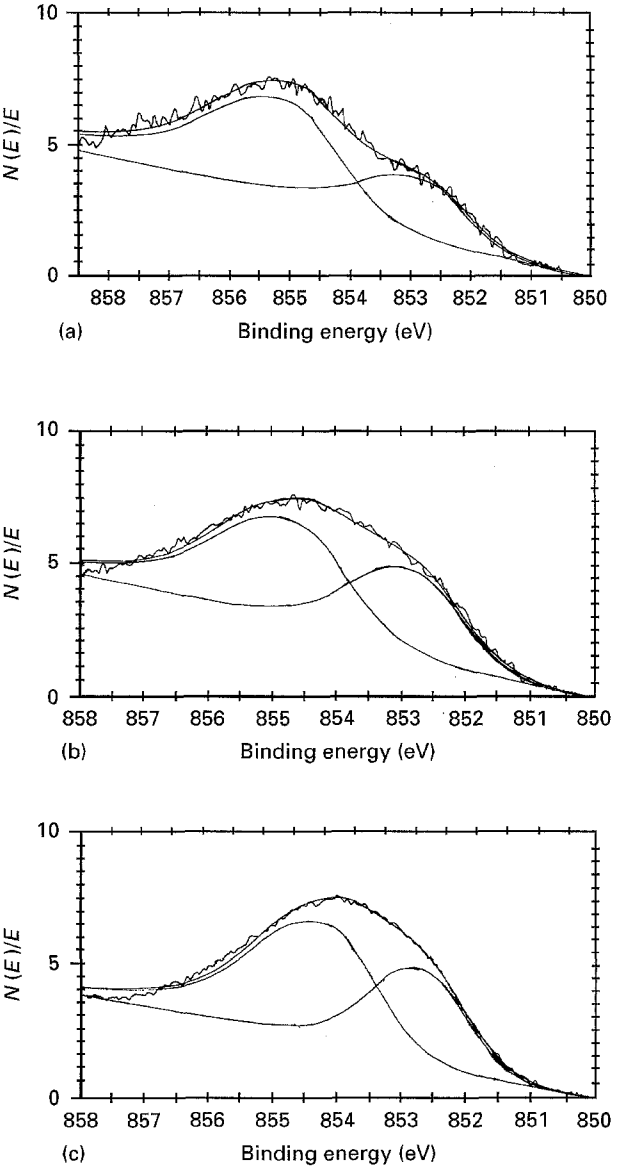

Figure 4 ESCA spectra of nickel and their deconvolutions to different valences of nickel ions: (a) the black precipitates before sintering; (b) the lithium nickel oxide ceramics after 4 h sintering; and (c) that after 11 h sintering.

TABLE III Deconvoluted ESCA spectra for nickel in the lithium nickel oxides

Element	Sintering time (h)	Peak position (eV)	FWHM[a]	Area (%)
Nickel	0	855.01	2.00	66.62
		852.78	1.61	33.38
	4	854.70	2.00	60.04
		852.84	1.83	39.96
	11	854.19	1.88	60.78
		852.69	1.74	39.22

* Full-width at half-maximum.

infrared spectra of the multi-phase precipitates were similar to those of single-phase $Li_{0.61}Ni_{0.96}O_{2.0}$ ceramics [15]. An additional band at 1084.6 cm^{-1} in the multi-phase precipitates did not appear in the sintered ceramics, suggesting a transition of the multi-phases

TABLE IV Electrical properties of the lithium nickel oxides sintered at 700 °C

Sample	Sintering times (h)	Temperature (°C)	Resistivity, ρ(Ω cm)	Conductivity $\sigma(\Omega^{-1}\,cm^{-1})$
Black ppt	0	30	296	3.4×10^{-3}
		100	89	1.1×10^{-2}
		200	15	6.7×10^{-2}
		250	11	9.1×10^{-2}
$Li_{0.61}Ni_{0.96}O_{2.0}$	4	30	197	5.1×10^{-3}
		100	39	2.6×10^{-2}
		200	13	7.7×10^{-2}
		250	10	1.0×10^{-1}
	11	30	5.0	2.0×10^{-1}
		100	1.8	5.6×10^{-1}
		200	0.89	1.1
		250	0.43	2.3

to single-phase lithium nickelate during thermal treatments.

3.5. Valence states of nickel

The mixed valence states of nickel were studied with the aid of ESCA. Fig. 4 reveals that little change in the nickel valences occurred as sintering times were increased, indicating no significant influence of the sintering processes on the nickel valences. The ESCA spectra of all products show a widened Ni $2p_{3/2}$ peak with a full-width at half-maximum of greater than 3.6 eV, which was characteristic of dual peaks (Fig. 4). The dual peaks could be deconvoluted into two peaks with integrated areas of approximate 60% at 854.7 eV and 40% at 852.8 eV, respectively. They were assumed to correspond to the Ni^{4+} and Ni^{3+} species, respectively. A semi-quantitative ratio of $Ni^{4+}:Ni^{3+}$ = 60:40 was obtained from the deconvoluted ESCA peaks of nickel. These ESCA results reveal that the oxidation reactions of the low valence Ni^{2+} species to high valences of Ni^{3+} and Ni^{4+} by H_2O_2 were completed before sintering processes, because deconvoluted peaks of the nickel ion revealed no big discrepancy among the products sintered from 0–11 h (Table III).

3.6. Conductivities

Table IV shows the conductivity of the $Li_{0.61}Ni_{0.96}O_{2.0}$ ceramics as a function of temperature. It reveals that the temperature has a strong influence on conductivity, i.e. conductivity increased as the temperature was raised. At 30 °C, the conductivities improved sharply from $3.4\times10^{-3}\,\Omega^{-1}\,cm^{-1}$ to $5.1\times10^{-3}\,\Omega^{-1}\,cm^{-1}$ to $2.0\times10^{-1}\,\Omega^{-1}\,cm^{-1}$ as the sintering times were increased from 0 to 4 to 11 h. Such a conductivity is suitable for use as electrode materials. This is consistent with the enhancement of the degree of ordering of the cations as the sintering durations increased.

4. Conclusion

Ordered nanophase $Li_{0.61}Ni_{0.96}O_{2.0}$ ceramics, with crystallite sizes in the range 80–200 nm, have been prepared through the soft chemical routes. The oxidation of Ni^{2+} to Ni^{3+} and Ni^{4+} species was completed during solution reactions at 50–60 °C and evaporation at 105–150 °C (strong oxidation stage). After the solution was evaporated to dryness, multiple-phase black precipitates were obtained, and then transformed to single-phase $Li_{0.61}Ni_{0.96}O_{2.0}$ ceramics by sintering. The single-phase $Li_{0.61}Ni_{0.96}O_{2.0}$ ceramics had a rhombohedral structure (space group R3*m*). As sintering times increased, the rhombohedral morphology of crystallites became more distinct and ordering of the cations between the layers was enhanced. Compared to the conventional ceramic and solution routes, sintering times in the soft chemical route were dramatically reduced ($\leqslant$ 11 h) even at 700 °C, while the nanophase $Li_{0.61}Ni_{0.96}O_{2.0}$ shows satisfactory conductivity for use as electrode materials.

Acknowledgements

This research was financially supported by the Foundation of Young Scientists established by the State Educational Commission of China. We thank Mrs Lizhu Ye for her help with the XRD analysis and Mr Youfa Zhu for the use of ESCA.

References

1. M. G. S. R. THOMAS, P. G. BRUCE and J. B. GOODENOUGH, *J. Electrochem. Soc.* **132** (1985) 1521.
2. T. OHZUKU, Y. IWAKOSHI and K. SAWAI, *ibid.* **140** (1993) 2490.
3. R. KANNO, H. KUBO, Y. KAWAMOTO, T. KAMIYAMA, F. IZUMI, Y. TAKEDA and M. TAKANO, *J. Solid State Chem.* **110** (1994) 216.
4. K. M. ABRAHAM, *Electrochimia Acta* **38** (1993) 1233.
5. J. M. TARASCON and D. GUYOMARD, *ibid.* **38** (1993) 1221.
6. S. J. VISCO and L. C. DE JONGHE, *ibid.* **38** (1993) 1157.
7. N. Q. MINH, *J. Power Sources* **24** (1988) 1.
8. P. G. BRUCE, A. LISOWSKA-OLEKSIAK, M. Y. SAIDI and C. A. VINCENT, *Solid State Ionics* **57** (1992) 353.
9. G. DUTTA, A. MANTHIRAM, J. B. GOODENOUGH and J. -C. GRENIER, *J. Solid State Chem.* **96** (1992) 123.
10. C. N. R. RAO and J. GOPALAKRISHNAN, *Acc. Chem. Res.* **20** (1987) 228.

11. A. ROUSSET, F. CHASSAGNEUX and J. PARIS, *J. Mater. Sci.* **21** (1986) 3111.
12. D. CHAKRAVORTY and A. K. GIRI, in "Chemistry of Advanced Materials", edited by C. N. R. Rao (Blackwell Scientific, Oxford, 1993), Ch. 10, p. 217.
13. The X-Ray Powder Diffraction Files **23-362** for $Li_{0.4}Ni_{1.6}O_2$, **14-483** for Ni_2O_3, **22-1189** for NiO.
14. E. ZHECHEVA and R. STOYANOVA, *Solid State Ionics* **66** (1993) 143.
15. T. OHZUKU, A. UEDA, M. NAGAYAMA, Y. IWAKOSHI and H. KOMORI, *Electrochimia Acta* **38** (1993) 1159.

Received 31 October 1995
and accepted 8 May 1996